LIGHT SCATTERING SIZE ESTIMATION OF NEARLY MONODISPERSE SPHERICAL PARTICLES IN THE MULTIVALUED REGION: A REMINISCENCE

Blahoslav SEDLÁČEK

Institute of Macromolecular Chemistry,
Czechoslovak Academy of Sciences, 162 06 Prague 6

Received July 16, 1988
Accepted September 26, 1988

Dedicated to Prof. Otto Wichterle on the occasion of his 75th birthday.

For the size estimation of large, nearly monodisperse spherical particles, the forward angle dissymmetry technique (FAD) has been used and the results compared with data obtained by the transmission electron microscopy (TEM) and integral turbidity ratio (ITR) methods. Starting with a certain relative particle size which depends on the chosen angle pair, the FAD functions go through several extremes and become multivalued. The possibility of the particle size estimation under such conditions and, also, without the knowledge of actual particle concentration (but knowing the relative refractive index), is discussed in this paper.

During the sixties, several excellent angular methods based on the Lorenz–Mie (L–M) theory were developed[1–9] and tested on latexes for further use in the characterization of polymer and biopolymer particles, colloids and gels. Whilst these techniques reached their zenith within a few years, another very powerful method originated at the same time started its giddy career – the photon correlation spectroscopy; it witnesses by its top qualities that this boom has been lasting until now. It seemed some time ago that the classical light scattering methods are almost superfluous, but now a symbiosis is seen as the most rational solution. Although the classical methods are rather minor partners in the majority of problems to be solved, there are regions where they can be used equivalently or preferentially.

This paper deals with spherical particles (as a model) and classical L–M techniques: especially the forward angle dissymmetry method[9,10] (FAD), being one of the so-called ratio methods, leads to a simple and rapid size estimation of (nearly) monodisperse particles with a plausible accuracy provided that their size does not exceed a certain limit, i.e. the first maximum of FAD.

If we have to do with large particles, we must expect the character of FAD to become much more complicated as the particle size increases. Usually, it is not easy to identify the size of large particles with a correct value of the parameter α explained

in Methods. Therefore, the purpose of this paper is to indicate under which conditions is it possible to estimate the particle size also in the multivalued region. Data thus obtained have been compared with results supplied by the electron microscopy and integral turbidity ratio (ITR) methods.

METHODS

Sample. A monodisperse polystyrene latex, kindly supplied by Dr Antl (Research Institute for Coating Materials, Prague) has been used in this study. The original suspension (1·0%) was diluted $10^2 \times$ (ITR) and $10^4 \times$ (FAD) with a stabilizer containing distilled water. The stock solutions thus obtained were further diluted according to the following schemes: ITR — 4 : 3 : 2 : : 1 (10^{-5} ml/ml); FAD — 2·67 : 2·00 : 1·33 : 0·67 (10^{-7} ml/ml). The diluent was purified by pressure filtration through a G5 fritted disc; of the latex samples, only the basic were purified by partial sedimentation. The samples for electron microscopy were taken directly from cells used in the light scattering measurements; samples were prepared repeatedly.

Transmission electron microscopy (TEM). A common replica technique was used for treating the specimens for electron microscopy. The particle size on photographic plates were measured with an Abbé comparator (Zeiss, Jena). Six sets of photographs (enlargement 13 000, 17 100 and 21 850) with many hundreds of particles were evaluated to obtain a more reliable picture of the monodispersity of particles.

Integral turbidity ratio method (ITR). The particle size estimation by means of the ITR method leads to relatively accurate and reliable results, being a somewhat different version of classical Wallach's[11] method of turbidity spectra. The turbidities τ are measured at wavelengths Λ_0 (435·8 nm), Λ_1 (546·1 nm) and Λ_2 (684·3 nm). Their ratios $T_{01} = \tau_0/\tau_1$, $T_{02} = \tau_0/\tau_2$, and $T_{12} = \tau_1/\tau_2$ are related to the relative (α) or absolute (L) particle size by a general equation

$$T_{ab} = \frac{\tau_a(\lambda_0\kappa^a, \alpha/\kappa^a, m)}{\tau_b(\lambda_0\kappa^b, \alpha/\kappa^b, m)} = \kappa^{-2(b-a)} \frac{S_a(\alpha/\kappa^a, m)}{S_b(\alpha/\kappa^b, m)},$$

where L is the particle diameter, λ is the wavelength in the medium (Λ/n), $\lambda_0 = 326{\cdot}7$ nm, $\alpha = \pi L/\lambda$ is the relative size of particles, $m = n'/n$ is the relative refractive index (n' and n being the refractive indices of the particle and system, respectively), and $\kappa = 1{\cdot}2531$ is the quotient of a sequence of wavelengths; the function S depends only on α and m, not on λ (for details see[12]). The desired particle size may be found from tables[12] or may be calculated in terms of the L–M theory.

A Perkin–Elmer–Hitachi spectrometer (Model 340) was used for transmission measurements of light scattering with rectangular cells of 10 mm depth. Normally, the three wavelengths given above were used for the estimation of turbidity, unless another set of wavelengths is to be preferred for an unambiguous choice of correct data.

Forward angle dissymmetry method (FAD). Most theoretical light scattering functions, used for the particle size estimation in monodisperse systems, have a distinctly oscillating character, especially, when the angular functions are considered. Except the angular intensity method for *single* particles[13,14] (where the experimental data are compared directly with the theoretical angular spectra using a computer data bank), all other methods dealing with particle systems give the angular spectra more or less deformed by "omnipresent" polydispersity. Slightly polydisperse systems were shown by many authors to be amenable to theoretical functions valid for

monodisperse system, but this is very limited in our case owing to the strong sensitivity of this method to latex polydispersity[9]. A deviation from uniformity can be detected by the variation of wavelength, the angle ratio, or both[9]. When working with a nearly monodisperse system of very large particles, one must expect a difficulty which hardly can be surmounted by using the oscillating functions. This problem, very similar to that of passing Scylla without falling victim to Charybdis, seems to be soluble only under favourable conditions.

The forward angle dissymetry is defined as a ratio ζ of the scattering intensities $i_{\theta 1}$ and $i_{\theta 2}$ at two angles θ_1 and θ_2. Thus we have $\zeta = i_{\theta 2}/i_{\theta 1}$ expressed by Maron's plot[9] for $i_{\theta 2}/i_{\theta 1}$; however, our plot for $i_{\theta 1}/i_{\theta 2}$, i.e. the reciprocal plot $\zeta = i_{\theta 1}/i_{\theta 2}$, is used in this paper. The interval between the individual angles in Maron's paper is usually 10°, while in this paper it is 15°. The L–M data have been calculated from tables[15] using $\theta_1/\theta_2 = 30/45$, 45/60 and 60/75 in unpolarized and polarized light. Measurements were carried out at green (546·1 nm) and blue (435·8 nm) wavelengths, which correspond to $\lambda_g = 409{\cdot}3$ and $\lambda_b = 326{\cdot}7$ nm in the milieu used, and thus the value of one α is 130·28 and 103·99 nm, respectively.

Scattering intensities have been measured with Sofica apparatus at angles 30, 45, 60 and 75° (FAD). As all angles are situated in the forward quadrant, experimental intensity ratios must be corrected for the volume seen by the photomultiplier; the following correction factors are to be used: 0·707 (30/45), 0·818 (45/60) and 0·897 (60/75).

The use of the forward angle dissymmetry method brings several advantages, the most important being: *1*) the FAD method enlarges considerably the extent of measurement, i.e. the first maximum (for $m = 1{\cdot}20$ and (30/45)) can be reached at $\alpha = 5{\cdot}1$, as compared with $\alpha = 2{\cdot}0$ obtained by classical dissymmetry (Debye's method); *2*) there is no need of absolute concentration data and extrapolation of relative data is quite satisfactory; *3*) also, a negligible dependence on the relative refractive index, m, makes possible the size estimation without precise knowledge of m provided that the particles are sufficiently small (for $m = 1{\cdot}20$ about $\alpha < 4$).

RESULTS AND DISCUSSION

Transmission Electron Microscopy (TEM)

The TEM method was used to collect independent data on the number-average particle size and its percent deviation. Data thus obtained are usually considered as a representative standard, which is however not well-deserved; therefore, we tried to reduce possibility of misleading observations (due to experimental errors and inadequate choice of objects) by measuring six independent sets of particle ensembles, some hundred particles each. The results given in Table I clearly show that the particles are nearly monodisperse; the extreme particle sizes differ only slightly from the average (by 0·76 to 1·73%). However, as only separate particles were measured, the presence of some contaminants (either real or fictitious) cannot be fully excluded in the whole sample. The reason for this may consist not only in *a*) an inaccurate enlargement of micrographs in the individual sets, but also in *b*) a low a priori polydispersity, *c*) small but possible aggregation (proceeding for different times in the stock solution, or changing during purification of samples), or *d*) combination of some individual factors. Unfortunately, this uncertainty can hardly be reduced, probably with the exception of item *a*).

Integral Turbidity Ratio Method (ITR)

The ITR method, shortly described in Methods, offers a very simple but adequate approach to the problem. The results thus obtained are presented in Table II: two

TABLE I

Particle size of polystyrene latex estimated by electron microscopy

Sample	nm	±nm	±%	Max.	Enlargement
1	773	13·3	1·73	809	13 000×
2	764	11·9	1·56	785	13 000×
3	800	6·6	0·83	810	17 100×
4	801	7·7	0·97	808	17 100×
5	776	5·9	0·76	786	17 100×
6	778	13·3	1·71	791	21 850×
Average	*782*	*9·8*	*1·26*	*798*	

TABLE II

Estimation of polystyrene latex particles by ITR method

c^a	τ_0/τ_1	τ_0/τ_2	τ_1/τ_2	α_{01}	α_{02}	α_{12}	L_{01}	L_{02}	L_{12}
c_1	1·275	1·821	1·428	8·08	7·87	7·64	840	818	795
c_2	1·278	1·826	1·428	8·03	7·85	7·64	835	816	795
c_3	1·284	1·835	1·429	7·93	7·79	7·59	825	810	789
c_4	1·292	1·846	1·431	7·83	7·73	7·54	814	804	784
$c_0{}^b$	1·295	1·853	1·432	7·78	7·70	7·70	805	800	780
$\bar{c}^c$	1·285	1·832	1·429	7·93	7·79	7·58	824	810	788
c_1	1·280	1·832	1·431	8·01	7·83	7·58	833	814	788
c_2	1·280	1·835	1·433	8·01	7·81	7·52	833	812	782
c_3	1·284	1·842	1·435	7·96	7·75	7·46	827	806	776
c_4	1·293	1·872	1·448?	7·81	7·61	7·17?	812	791	746?
$c_0{}^b$	1·290	1·853	1·438	7·90	7·70	7·32	808	800	761
$\bar{c}^c$	1·284	1·845	1·436	7·93	7·74	7·41	823	805	771

[a] Concentration of particles (even if exact data not needed for estimation), $c_1 = 4 \cdot 10^{-5}$ ml/ml, further diluted in the sequence 4 : 3 : 2 : 1; [b] c_0 and $\bar{c}$, respectively, are the related "concentrations", corresponding to that extrapolated (for $c \to 0$) and to that being an average of data, i.e. to extrapolated or averaged ratios of τ_0/τ_1, etc. or of α_{01}, etc.

independent measurements were made. The individual ratios (τ_0/τ_1; τ_0/τ_2; τ_1/τ_2) differ almost negligibly from each other and it seems that they are not concentration dependent; however, a small trend can be recognized and thus respected in the individual columns, especially when extrapolated to zero concentration. Data expressed in α's and L's (where L is given in nm) were taken from tables published some time ago[12]. The results obtained for both measurements are very similar, while the data extrapolated (c_0) or averaged ($\bar{c}$) are intrinsically almost identical (see Table II). As expected, data for $\bar{c}$ are higher than those for c_0 due to extrapolation of c_0-data to zero concentration, which are always lower:

$$L(\text{for } c_0)\text{: } 807;\ 800;\ 771 \text{ nm}$$
$$L(\text{for } \bar{c})\text{: } 823;\ 808;\ 780 \text{ nm}.$$

This is not necessarily a measure of the whole polydispersity of the sample: indeed, a very small portion of aggregates or other contaminants could be responsible for the effect observed. However, the unequal response of the individual ratios in each triad, decreasing in the sequence L_{01}, L_{02} and L_{12}, gives evidence about the presence of some large particles in the system. It is interesting, even if not persuasive, that each of the triads covers the particle system nearly from the weight average to the number average.

Forward Angle Dissymmetry Method: Exposition

Here, it is perhaps necessary to recall Fig. 1 for better understanding the ITR and FAD functions. At the bottom, a graph (in two parts) of the ITR function is presented, concerning the region from $\alpha = 0$ to $\alpha = 20$ (for $m = 1{\cdot}20$ and wavelength ratio 435·8/546·1 nm). The other graphs of the FAD function are presented above, also in two parts; only graphs for angle ratios 30°/40°, 45°/60° and 60°/75° (unpolarized light) are given. Insets in the graphs show how complicated in details the curves are. For situating graphs in this figure correctly, it is useful to know the limiting values of ζ for $\alpha = 0$; also, the remaining data for polarized components are given here (u unpolarized, v vertically and h horizontally polarized).

Polarization	30°/45°	45°/60°	60°/75°
u	1·16̇	1·20	1·17
v	1·00	1·00	1·00
h	1·50	2·00	3·73

A suitable approach should be found for obtaining adequate data about large particles by the FAD method, which makes the extrapolation of steep and curved data trustworthy. To avoid multivalued results, a simple but probably the best

solution is to extend the region preceding the first maximum. This can be achieved[9] by *a*) shifting the measurements to smaller angles and *b*) using a lower difference between angles (e.g. 10° or less). The effect obtained can be seen in a considerable extension of a maxima-free domain, but partly at the price of a lower accuracy of both estimations. In practice, this process cannot exceed a certain limit.

However, this paper should check whether it is possible to make an adequate estimation also within the multivalued region. Therefore, conditions have been chosen where the number of extremes in a given region (2 or 2·5 μm) reaches one to eight maxima. The system is considerably complicated by the coexistence of several factors: in addition to the influence of the low remaining polydispersity, thermodynamic and optical problems play the most important part here. The results ob-

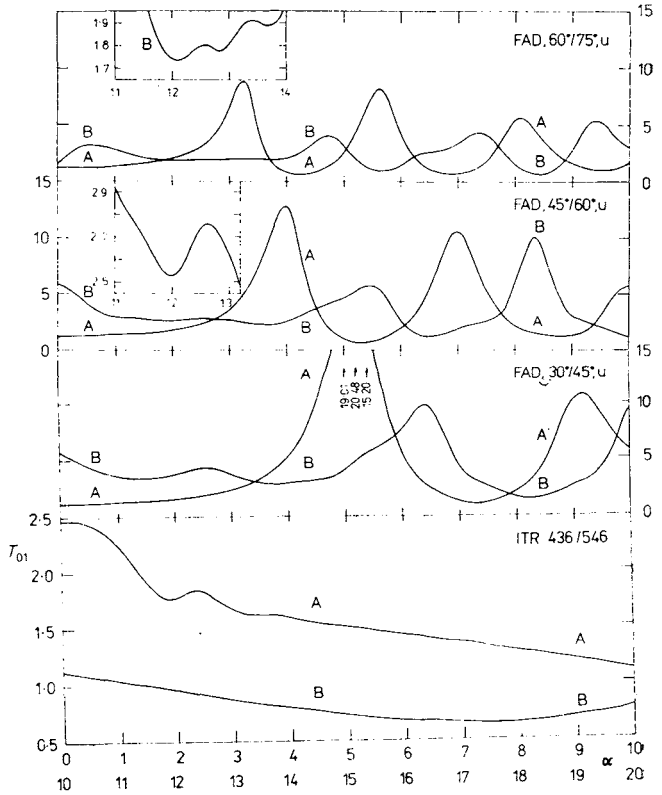

FIG. 1

Graphs of the ITR and FAD methods for the intervals $\alpha = 0-10$ and $10-20$. $\alpha = \pi L/\lambda$; $T_{01} = \tau_0/\tau_1$; $\zeta = i_{\Theta 1}/i_{\Theta 2}$ for 30°/45°, 45°/60° and 60°/75°. A and B correspond to the first and the second part of the graph, respectively. Insets are located in FAD, 45°/60° and 60°/75°

TABLE III

Particle size (L, nm) estimation by the FAD method: extrapolation of scattering ratios ζ for $c \to 0$ (unpolarized light, 546·1 nm)

c[a]:	c_1	c_2	c_3	c_4	c_0[c]	α[d]	c_1	c_2	c_3	c_4	c_0[c]	α[d]	c_1	c_2	c_3	c_4	c_0[c]	α[d]
ζ[b]:	1·46	1·44	1·41	1·38	1·38		6·08	6·28	6·12	5·33	5·10		1·00	0·96	0·97	0·99	0·93	
	$\theta_1/\theta_2 = 30°/45°$						$\theta_1/\theta_2 = 45°/60°$						$\theta_1/\theta_2 = 60°/75°$					
A	241	232	224	210	—	—	—	—	—	—	—	—	—	—	—	—	—	—
B	—	—	—	—	—	—	440	443	440	429	—	—	—	—	—	—	—	—
C	—	—	—	—	—	—	—	—	—	—	—	—	509	511	510	509	—	—
D	—	—	—	—	—	—	565	565	565	572	—	—	—	—	—	—	—	—
E	—	—	—	—	—	—	—	—	—	—	—	—	600	596	598	599	—	—
F	895	898	899	903	904	6·94	853	855	853	846	842	6·46	855	857	856	855	859	6·59
G	1 008	1 007	1 005	1 002	999	7·67	967	965	967	976	981	7·53	943	941	942	963	939	7·27
H	—	—	—	—	—	—	—	—	—	1 280	—	—	—	—	—	—	—	—
I	—	—	—	—	—	—	—	—	—	1 332	—	—	—	—	—	—	—	—
J	—	—	—	—	—	—	—	—	—	1 984	—	—	2 019	2 024	2 022	2 020	—	—
K	—	—	—	—	—	—	—	—	—	2 037	—	—	2 061	2 059	2 060	2 061	—	—
L	2 357	2 361	2 365	2 373	2 384	18·3	2 344	2 345	2 345	2 340	2 331	17·9	2 364	2 367	2 366	2 364	2 367	18·2
M	2 404	2 401	2 400	2 388	2 437	18·7	2 432	2 430	2 332	2 439	2 444	18·8	2 436	2 430	2 432	2 435	2 329	18·7

[a] Concentration of particles expressed in 10^{-7} g/g: c_1 (2·44), c_2 (1·83), c_3 (1·22), c_4 (0·61), i.e. diluted in the sequence 4 : 3 : 2 : 1; [b] $\zeta = i_{\theta_1}/i_{\theta_2}$ (intensity ratio at angles θ_1 and θ_2); [c] c_0 is the related "concentration", corresponding to the extrapolated value (for $c \to 0$) expressed also in [d] $\alpha = \pi L/\lambda$.

tained, which are not easy to survey, are experimental in nature, i.e. not enough supported by some theoretical approach. Data presented here are only a small portion of those measured, but sufficient to understand better the method, at least experimentally.

Particle Size Estimation by FAD *Method*

It is well-known[9] that the concentration dependence of the FAD method may be conspicuously curved; it is therefore always necessary to extrapolate the data obtained to zero concentration. In Maron's notation[9] the values increase with concentration: this means that in our "reciprocal" notation the values must decrease. This was however not the case in many of our observations. To explain such a discrepancy, one should take into account that Maron's measurements are situated prior to the first extreme (maybe except the largest particles), and thus his finding is adequate, approaching the extreme from the left side (ascending branch). If we deal with the opposite side of the extreme (descending branch), the situation is different: we must reckon with either increasing or decreasing trends in the concentration dependence and, necessarily, also rather compensated forms are to be expected. All such forms can be seen in Table III.

However, to demonstrate this dependence to be valid, we have chosen another approach than that used by Maron. In addition to the extrapolation of ζ against c (in our notation), we used that of α or L against c, the latter being shown in Table III. In all measurements, using the green and blue light, polarized or unpolarized, the emerging picture was nearly the same; accordingly, only one example is given from the numerous measurements made. This extrapolation seems to be much less steep and curved, and often is found to be nearly quite compensated. The reason for this may be derived from the observation that, in the region of steep maxima, a relatively large change in ζ corresponds to a very small change in α or L. In turn, this might also explain (at least in part) that ζ may have lower value than expected (see Table III, 45/60 compared with 60/75), probably as a result of a not quite accurate measurement, especially in the vicinity of extremes. Moreover, being in the region with the almost compensated behaviour, the data obtained are practically identical.

It should be elucidated now by checking the individual factors whether the concentration dependence only could be used for independent elimination of false choice from two, four or six possible solutions (e.g. see Table III). For this purpose, Table IV collects data obtained for 546·1 and 435·8 nm, either unpolarized or polarized (v). These data are expressed in $\alpha = \pi L/\lambda$, extrapolated for $c \to 0$, i.e. α_0^ζ, in L_0^ζ (extrapolation of ζ against c) and in L_0 (extrapolation of L against c); only the first two data (row 1, 2) in each blocks (A – D) have been taken into account. One can see that almost all "unpolarized" data are compensated, i.e. L_0^ζ and L_0 data are practically identical. The vertically polarized data are compensated only partly,

TABLE IV

Particle size (L, nm) estimation by FAD method: abbreviated data for a set of measurements at 546·1 and 435·8 nm, both with unpolarized (u) and vertically (v) polarized light

λ	θ_1/θ_2 30°/45°			45°/60°			60°/75°			Blocks Rows
	α_0^{ζ} [a]	L_0^{ζ}, nm [b]	L, nm [c]	α_0^{ζ} [a]	L_0^{ζ}, nm [b]	L, nm [c]	α_0^{ζ} [a]	L_0^{ζ}, nm [b]	L, nm [b]	
	$\zeta_0 = 1{\cdot}38$		—	$\zeta_0 = 5{\cdot}10$		—	$\zeta_0 = 0{\cdot}93$		—	A
	6·94	904	904	6·46	842	844	6·59	859	854	1
546	7·67	999	998	7·53	981	980	7·21	939	942	2
(u)	18·3	2 384		17·9	2 331		18·2	2 367		3
	18·7	2 437		18·8	2 444		18·7	2 429		4
	$\zeta_0 = 1{\cdot}03$		—	$\zeta_0 = 7{\cdot}80$		—	$\zeta_0 = 0{\cdot}60$		—	B
	6·61	861	900	6·31	821	840	6·54	852	841	1
546	7·64	995	966	7·38	961	968	7·21	939	944	2
(v)	18·2	2 365		17·9	2 328		18·0	2 351		3
	18·3	2 380		18·7	2 440		18·7	2 430		4
	$\zeta_0 = 5{\cdot}01$		—	$\zeta_0 = 1{\cdot}40$		—	$\zeta_0 = 1{\cdot}49$		—	C
	8·51	885	890	8·40	874	868	7·41	771	768	1
436	10·3	1 070	1 020	9·13	950	955	9·07	943	936	2
(u)	19·6	2 037		20·0	2 082		20·8	2 162		3
	21·2	2 208		20·4	2 120		21·5	2 234		4
	$\zeta_0 = 5{\cdot}50$		—	$\zeta_0 = 1{\cdot}03$		—	$\zeta_0 = 1{\cdot}28$		—	D
	8·46	880	879	8·35	868	864	8·97	933	771	1
436	10·1	1 048	1 020	9·13	949	951	9·92	1 032	932	2
(v)	19·5	2 029		17·9	2 053		18·8	1 955		3
	21·2	2 204		20·4	2 117		20·6	2 141		4

[a] α_0^{ζ} and [b] L_0^{ζ} are, respectively, extrapolated values of α^{ζ} and L^{ζ} (for $c \to 0$), superscript ζ indicating extrapolation to occur via ζ against c; [c] another extrapolation is that of L against c.

i.e. the correlation between blocks u and v is rather poor, but it must be taken into account that the deviations are relatively low, usually less than 5%, rarely more.

TABLE V

Theoretical FAD data for $\alpha_g = 6{\cdot}60$, $7{\cdot}40$, $8{\cdot}00$ and $\alpha_b = 8{\cdot}27$, $9{\cdot}27$, $10{\cdot}02$. (Is the solution unambiguous?)

Block	Unpolarized (u)			Vertical (v)			Horizontal (h)		
	30°/45°	45°/60°	60°/75°	30°/45°	45°/60°	60°/75°	30°/45°	45°/60°	60°/75°
				860 nm ($\alpha_g = 6{\cdot}60$)[b]					
ζ[a]	2·12	6·77	0·90	1·66	10·47	0·46	2·71	4·66	2·01
1	*860*	*860*	*860*	*860*	*860*	*860*	*860*	*860*	*860*[d]
2	1 043	958	938	1 032	945	930	1 066	988	988
3	2 309	2 348	2 369	2 316	2 342	2 354	2 291	2 360	2 356
4	2 447	2 425	2 429	2 426	2 426	2 427	2 474	2 437	2 469
				860 nm ($\alpha_b = 8{\cdot}27$)[c]					
ζ[a]	3·25	1·57	5·15	3·50	1·15	7·80	3·04	2·26	3·26
5	*860*	*860*	*860*	*860*	*860*	*860*	*860*	*860*	*860*[d]
6	—	956	—	—	955	—	—	979	—
7	2 250	2 125	—	2 236	2 121	2 257	2 272	2 148	—
8	2 440	—	—	2 425	2 290	2 325	2 451	2 407	2 315
				964 nm ($\alpha_g = 7{\cdot}40$)[b]					
ζ[a]	1·12	6·37	1·42	0·78	7·18	1·22	1·51	5·62	1·68
a	942	856	833	—	846	823	—	881	883
b	*964*	*964*	*964*	*964*	*964*	*964*	*964*	*964*	*964*[d]
c	—	—	1 186	—	—	1 171	—	—	—
d	—	2 346	2 345	—	2 331	2 332	—	—	2 374
e	—	2 431	2 448	—	2 437	2 448	—	2 397	2 452
				964 nm ($\alpha_b = 9{\cdot}27$)[c]					
ζ[a]	10·57	1·80	1·20	15·00	1·53	0·77	7·85	1·90	2·04
f	942	847	763	925	840	758	946	874	790
g	*964*	*964*	*964*	*964*	*964*	*964*	*964*	*964*	*964*[d]
h	—	—	1 019	—	—	1 021	—	—	1 080
i	2 130	2 175	—	—	2 127	2 157	—	2 131	2 178
j	—	2 227	—	2 219	2 287	2 226	—	—	2 265

TABLE V
(*Continued*)

Block	Unpolarized (u)			Vertical (v)			Horizontal (h)		
	30°/45°	45°/60°	60°/75°	30°/45°	45°/60°	60°/75°	30°/45°	45°/60°	60°/75°
				1 042 nm (α_g = 8·00)[b]					
ζ[a]	2·10	2·20	5·56	1·98	1·73	13·23	2·20	2·93	2·94
A	861	787	770	843	783	759	881	818	816
B	*1 042*	*1 042*	*1 042*	*1 042*	*1 042*	*1 042*	*1 042*	*1 042*	*1 042*[d]
C	—	—	—	—	1 212	—	—	1 253	1 135
D	2 310	2 246	—	2 302	2 225	—	2 328	2 300	—
E	2 447	2 532	—	2 439	2 534	2 516	2 446	2 491	2 514
				1 042 nm (α_b = 10·02)[c]					
ζ[a]	5·81	5·78	1·70	5·69	9·14	1·76	5·94	4·14	1·63
F	—	775	775	—	761	776	—	—	764
G	896	1 037	933	882	1 071	917	911	799	1 007
H	*1 042*	*1 042*	*1 042*	*1 042*	*1 042*	*1 042*	*1 042*	*1 042*	*1 042*[d]
I	—	—	—	—	—	1 203	—	1 078	—
J	2 184	2 182	2 151	2 185	2 172	2 126	2 141	2 192	2 204
K	—	1 118	2 239	—	2 213	2 241	—	2 236	2 240

[a] $\zeta = i_{\theta 1}/i_{\theta 2}$, size of particles expressed in $\alpha = \pi L/\lambda$; [b] α_g (green light); [c] α_b (blue light); [d] basic data are in italics.

Another complication occurs when going to larger particles. For smaller particles the data expressed in α are very similar for the two neighbouring scales, e.g. $m = 1{\cdot}15$ and $m = 1{\cdot}20$; under such conditions the differences (in parentheses) are as follows: $2{\cdot}0\alpha$ (0·0003), $3{\cdot}0\alpha$ (0·0426) and $4{\cdot}0\alpha$ (0·2424). However, in the region of large particles the differences become irregular (sometimes negative because of disturbed coincidence): $10{\cdot}0\alpha$ ($-1{\cdot}1225$), $15{\cdot}0\alpha$ (0·8142), $20{\cdot}0\alpha$ (6·0896) and $25{\cdot}0\alpha$ ($-1{\cdot}5963$). It is no longer valid that the FAD function can be used in a broad region of refractive indices; rather, the opposite is true, except in the nearest neighbourhood of the reference function given in the tables[10].

The situation is quite opposite with regard to the coincidence of extremes for unpolarized and vertically or horizontally polarized light: it is almost perfect over the whole region from $\alpha = 0$ to $\alpha = 25$, and the peaks coincide within the step of the tables ($\Delta\alpha = 0{\cdot}2$). There is no possibility to distinguish the right solution from those available.

FAD *Identity Problem*

To identify the correct solution among many solutions available in the multivalued region, we compiled theoretical data for selected particle sizes, i.e. 860 nm (α_g = 6·60, α_b = 8·27), 964 nm (α_g = 7·40, α_b = 9·27), and 1 042 nm (α_g = 8·00, α_b = 10·02)*; these data are very similar to those which appeared in Table IV and V (and those not published *in extenso*). All data are related to the respective sizes (i.e. 860, 964 or 1 042 nm) of particles which are considered as perfectly monodisperse. This approach was selected with the aim to find some distinction between the right solution and those inadequate. It revealed also some difference between the results for green (546·1 nm) and blue (435·8 nm) light used in individual measurements.

Three sets of data (double blocks 1–8, a–j, A–K) are presented in Table V, divided into two parts (blocks) and referring either to the green or blue light, polarized or unpolarized. The first block (1–4, 860 nm) differs considerably from all other blocks in that it encompasses complete data for polarized and unpolarized light. While the first row is constant (selected standard), the second row has a decreasing character, i.e. the apparent size of particles decreases with a sequence 30°/45°, 45°/60° and 60°/75° within each triad. However, the triads themselves have a different sequence: u–h–v. Other rows (3 and 4) are very consistent, either slightly increasing or decreasing. The second block (5–8; blue light) differs considerably from the preceding case: one can see that the data in rows 6–8 are not complete, i.e. the basic row 5 is the only solution.

The next double block (a–j) deals with the size of 964 nm. Owing to many "vacancies", only f and g can be taken into account. All individual triads have a decreasing character, but these triads themselves have a different sequence: h – u – v. We can see that, by analogy to the preceding case (see 1, 2), the data in f are too much disturbed and cannot be accepted.

A similar situation pertains also to the third double block (A–K). Data in A are disturbed with respect to G, having a sequence h – u – v; the remaining data are incomplete and thus incompetent. Data in F, I, and K are incomplete and may be cancelled; further, a disturbance in G (the sequence being not rational) leads to annulation of these data. Only J is acceptable and could be taken into account.

Now, it would be useful to confront theoretical data with those obtained from the experiment. If we compare Table V (row 1) with Table III (column 60°/75°, F), one can see that the data are nearly identical; however, the data in column 30°/45°, F (Table III) are not much but distinctly higher, probably due to some polydispersity present in the sample. Row 2 (Table V) shows that the polydispersity could not be too high, because the data are nearly the same as those in Table III, G.

* Here g and b stand for green and blue, respectively, when dealing with monodisperse particles.

TABLE VI

Particle size estimation by FAD method: test of adequacy. $\zeta = i_{\theta_1}/i_{\theta_2}$, ζ_g for green (546 nm) and ζ_b for blue (436 nm) light. α_g^l and α_b^l are, respectively, the relative particle sizes ($\alpha = \pi L/\lambda$) related to lower (l) data (see Table III, row F) for green and blue light; $\alpha_{bg}^l = \alpha_b^l/1{\cdot}2531$, which represents the deviation of "green data" from "blue data", expressed also in %. Similarly, data with superscript H are related to higher data (see row G of the same Table)

Block	30°/45°				45°/60°				60°/75°			
	c_1	c_2	c_3	c_4	c_1	c_2	c_3	c_4	c_1	c_2	c_3	c_4
					Unpolarized light							
ζ_g	1·46	1·44	1·41	1·38	6·08	6·28	6·12	5·33	1·00	0·96	0·97	0·99
ζ_b	5·74	6·09	6·14	5·42	1·54	1·53	1·53	1·45	1·96	1·90	1·75	1·61
α_g^l	6·87	6·90	6·91	6·93	6·55	6·56	6·55	6·49	6·56	6·58	6·57	6·56
α_b^l	8·59	8·62	8·63	8·56	8·28	8·28	8·29	8·34	7·51	7·53	7·49	7·44
α_{bg}^l	6·85	6·88	6·88	6·83	6·61	6·61	6·62	6·65	5·99	6·01	5·98	5·94
%	0·29	0·22	0·36	0·14	−0·92	−0·76	−0·92	−2·50	8·69	8·66	8·98	9·45
α_g^H	7·74	7·73	7·72	7·69	7·42	7·41	7·42	7·49	7·24	7·22	7·23	7·24
α_b^H	10·04	9·94	9·93	10·15	9·18	9·18	9·18	9·17	8·88	8·90	8·95	9·00
α_{bg}^H	8·01	7·93	7·92	8·10	7·33	7·33	7·33	7·33	7·08	7·10	7·14	7·18
%	−3·49	−2·65	−2·66	−5·33	1·21	1·08	1·21	2·14	2·21	1·66	1·24	0·83
					Vertically polarized light							
ζ_g	1·12	1·12	1·11	1·07	7·37	7·97	7·89	7·87	0·63	0·57	0·62	0·72
ζ_b	6·64	7·07	7·07	5·75	1·16	1·13	1·07	1·09	1·77	1·61	1·55	1·40
α_g^l	6·87	6·87	6·88	6·93	6·49	6·52	6·52	6·42	6·52	6·55	6·53	6·48
α_b^l	8·55	8·57	8·58	8·49	8·27	8·29	8·30	8·30	7·47	7·46	7·44	7·42
α_{bg}^l	6·82	6·84	6·84	6·87	6·60	6·61	6·62	6·62	5·96	5·95	5·94	5·92
%	0·73	0·44	0·58	0·87	−1·69	−1·38	−1·53	−3·12	8·59	9·16	9·03	8·64
α_g^H	7·71	7·73	7·70	7·67	7·39	7·34	7·37	7·41	7·21	7·20	7·21	7·25
α_b^H	9·84	9·78	9·78	9·98	9·18	9·23	9·17	9·17	8·82	8·87	8·88	8·93
α_{bg}^H	7·85	7·80	7·80	7·96	7·33	7·36	7·32	7·32	7·04	7·08	7·09	7·13
%	−1·82	−1·03	−1·30	−3·78	0·81	−0·27	0·68	1·21	2·36	1·67	1·66	1·66

[a] Concentration of particles, see Table III.

The concentration dependence along with the combination of green and blue light and the use of unpolarized and polarized light, are certainly good approaches to the problem studied. Table VI was therefore prepared using experimental data from Tables III and IV (and those not given explicitly). Here, α^{l} relates to lower values of α (e.g. Table III, F) and α^{H} to higher values of α (e.g. Table III, G) of each couple; $\alpha^{\mathrm{l}}_{\mathrm{bg}} = \alpha^{\mathrm{l}}_{\mathrm{b}}/1{\cdot}2531$ are data calculated on the basis of $\alpha^{\mathrm{l}}_{\mathrm{b}}$, the results being compared with the original $\alpha^{\mathrm{l}}_{\mathrm{g}}$ data. The difference between $\alpha^{\mathrm{l}}_{\mathrm{g}}$ and recalculated data from $\alpha^{\mathrm{b}}_{\mathrm{g}}$ is expressed in %. Similarly, data with superscript H lead to results for a higher particle size (usually, on the descending branch of a peak).

Inspection of Table VI leads to the conclusion that the behaviour of data for unpolarized and polarized light is very similar, showing increased per cent deviations in the same place in both parts of this table. The most striking is the appearance of deviations in the sixth row of the third column in either part of the table. Explanation of such observations is difficult. More light can be thrown when seeking the positions of the respective intersects in Fig. 1: in our case, for a size around $\alpha = 7$, the graphs show that they have a broad and gentle minimum (for 30°/45° and 60°/75°) or a steep peak (for 45°/60°). As the former are very shallow, each error in the ordinate brings about a great shift in the abscissa; the opposite is valid for the case 45°/60°, where some change in the ordinate leads to a very small change in the abscissa, which is decisive for the size measurement. (Still, we must accent that the errors reach 10% only quite exceptionally, usually being less than 1–2%.) Moreover, the horizontal instability of data in minima and the vertical instability in maxima may lead to deformations and thus not quite adequate results.

CONCLUSIONS

1. Data obtained for *perfectly monodisperse* particles can, in principle, be distinguished from each other and identified as the only solution to the problem provided that the measurements are made at two or more wavelengths (see Table V).

2. *Nearly monodisperse* particles can be estimated in the following steps: *a*) Usual measurement by the FAD method; *b*) collection and identification of possible solutions to the problem; *c*) calculation of the FAD functions for the most probable solutions; *d*) selection of the most probable data on the basis of comparison between experimental and theoretical functions. The most powerful selection is that leading to elimination of inadequate data by using two or more wavelengths or FAD ratios; also, elimination of the most disordered data in sequences may be useful.

3. It cannot be excluded that the FAD functions are always unambiguous. In such a case, two additional suitable techniques are recommended: *1*) Angle ratio variation[9] and *2*) use of another technique, like the ITR method: after situating roughly the order of the particle size by the ITR method, the FAD method can be used with much higher sensitivity (by two orders of magnitude).

The author is indebted to Dr F. Lednický for electron micrographs and to Mrs E. Šimáčková for technical assistance.

REFERENCES

1. Nakagaki M., Heller W.: J. Chem. Phys. *32*, 835 (1960).
2. Pangonis W. J., Heller W., Economou N. A.: J. Chem. Phys. *34*, 960 (1961).
3. Heller W., Pangonis W. J., Economou N. A.: J. Chem. Phys. *34*, 971 (1961).
4. Stevenson A. F., Heller W., Wallach M. L.: J. Chem. Phys. *34*, 1789 (1961).
5. Heller W., Tabibian R.: J. Phys. Chem. *66*, 2059 (1962).
6. Bhatnagar H. L., Heller W.: J. Chem. Phys. *40*, 480 (1964).
7. Heller W.: J. Chem. Phys. *40*, 2700 (1964).
8. Maron S. H., Pierce P. E., Elder M. E.: J. Macromol. Sci., Phys., B *1*, 28 (1967).
9. Maron S. H., Pierce P. E.: J. Polym. Sci. *27*, 183 (1969).
10. Sedláček B.: Collect. Czech. Chem. Commun. *35*, 2625 (1971).
11. Wallach M. L., Heller W., Stevenson A. F.: J. Chem. Phys. *34*, 1796 (1961).
12. Sedláček B., Verner B., Bárta M., Zimmermann K.: Collect. Czech. Chem. Commun. *44*, 2064 (1979).
13. Gucker F., Egan J.: J. Colloid Sci. *16*, 68 (1961).
14. Tůma J.: *Thesis. Optical Properties of Aerosols and Light Scattering on Individual Particles*. Czech Technical University, Prague 1980.
15. Denman H. H., Pangonis W. J., Heller W.: *Angular Scattering Functions for Spheres*. Wayne State University Press, Detroit 1966.

Translated by the author.